

Photoluminescence studies on Si-doped GaAs/Ge

M. K. Hudait^{a)}

Materials Research Centre, Indian Institute of Science, Bangalore-560 012, India and Central Research Laboratory, Bharat Electronics, Bangalore-560 013, India

P. Modak and S. Hardikar

Central Research Laboratory, Bharat Electronics, Bangalore-560 013, India

S. B. Krupanidhi^{b)}

Materials Research Centre, Indian Institute of Science, Bangalore-560 012, India

(Received 21 October 1997; accepted for publication 14 January 1998)

Photoluminescence (PL) spectroscopy has been used to study the silicon incorporation in polar GaAs on nonpolar Ge substrates. Shifts of PL spectra towards higher energy with growth temperature, trimethylgallium (TMGa) and arsine (AsH_3) mole fractions were observed. The full width at half maximum increases with increasing growth temperature, AsH_3 and TMGa mole fractions. The peak at 1.49 eV has been attributed to band-to-acceptor transition involving residual carbon. The PL peak energy shifts towards higher energy with increasing growth temperature due to the increase in electron concentration. A vacancy control model may explain the PL shift towards higher energy with increasing AsH_3 mole fraction. The PL peak shifts towards higher energy with increasing TMGa mole fraction. The experimental results about the growth temperature, trimethylgallium, and arsine mole fractions on silicon-doped GaAs on GaAs were presented for comparison. The outdiffusion of Ge into the GaAs epitaxial layer was hardly to be seen from the secondary ion mass spectroscopy result. © 1998 American Institute of Physics.

[S0021-8979(98)05108-1]

I. INTRODUCTION

GaAs/Ge epitaxial heterostructures (HSs) have received much attention as starting materials for the fabrication of photovoltaic devices^{1–6} and the potential application in electronic and optoelectronic devices.^{7–9} The high hole mobility of Ge, as well as its narrow band gap make the GaAs/Ge heterojunction suitable for the fabrication of *p*-channel field-effect transistors, phototransistors, and quantum confinement devices.^{9,10} Owing to its high mechanical strength, Ge is an optimized substrate material in terms of the power-to-weight ratio for high efficiency GaAs/Ge photovoltaic devices.^{11,12} As large-area, minority-carrier devices, III–V/Ge cells are extremely sensitive to defects. Thus, elimination of antiphase domains (APDs), which are characteristics of the polar-on-nonpolar epitaxy, and suppression of large-scale interdiffusion across the GaAs/Ge heterointerface remain as key challenges for increased yield, reliability, and performance.

The Si-doped GaAs on Ge, i.e., polar-on-nonpolar substrates by metal–organic vapor-phase epitaxy (MOVPE) is an important issue of the optical and electrical properties not only from a fundamental understanding but also for the device applications, such as the buffer and base layer of solar photovoltaic devices. The deposition of GaAs on Ge basically has the same problems as the epitaxial growth of layers with different lattice constants (e.g., InGaAs on InP).¹¹ How-

ever, in this case, there are two other problems to be tackled, i.e., the creation of APDs between the polar GaAs and the nonpolar Ge,^{13–21} and the interdiffusion of Ga, As, and Ge across the semiconductor interface.^{15,22–24} The surface preparation seems to be the most critical parameter that affects the quality of the growth morphology. To avoid the formation of APDs, harmful to photovoltaic performance as they reduce the short-circuit current, misoriented substrates were used. A further optimization of the GaAs growth conditions on Ge is needed for the reduction of the element interdiffusion across the GaAs/Ge interface. The main problem is to reduce the Ga diffusion into the Ge substrate to avoid the formation of an unwanted *p*–*n* junction that could affect the performance of the GaAs/Ge solar photovoltaic devices.⁶ Suppression of these APDs is the major obstacle to the realization of device quality GaAs/Ge structures. The lattice constant and the thermal expansion coefficient of Ge are very close to those of GaAs layer growth on a Ge substrate, giving the essential knowledge about the suppression of this antiphase disorder. With the advancement of molecular beam epitaxy (MBE), Ge was successfully grown on GaAs.²⁵ The reverse (GaAs/Ge), although it had device applications,^{24,26,27} proved much more difficult. Attempts to grow Ge/GaAs superlattices by MBE have shown that GaAs grows in islands on (100) Ge resulting in APD.²⁸ GaAs grown on (100) Ge by vapor-phase epitaxy (VPE), also shows APDs.¹⁸ A detailed study of the optimal growth conditions for APDs-free GaAs growth on Ge by metal–organic chemical-vapor deposition (MOCVD) has recently been reported by Li and co-workers.^{13,14} They

^{a)}Electronic mail: mantu@mrc.iisc.ernet.in

^{b)}Author to whom correspondence should be addressed. Electronic mail: sbk@mrc.iisc.ernet.in

find that a combination of a large substrate offset toward an in-plane $\langle 110 \rangle$ coupled with a high substrate temperature ($\sim 650^\circ\text{C}$ or higher), relatively low growth rate (below $2\mu\text{m/hr}$), and a high As/Ga ratio ($\sim 60:1$) are the requirements for APD-free MOCVD GaAs.¹⁴ No electrical doping measurement were done on these films, but evidence for massive Ge outdiffusion into GaAs grown on Ge by MOCVD at high growth temperatures and low growth rates has been previously reported,¹⁵ with the Ge outdiffusion being sufficient to produce a Burstein–Moss (bandfilling) shift in the room-temperature photoluminescence (PL) spectra of thick layers, and to affect the x-ray rocking curves of thin layers. Since Ge diffusion into GaAs occurs via Ga vacancies¹⁵ and the Ga vacancy population will increase with increasing V/III ratio and with decreasing growth rate (i.e., lower Ga flow), it appears that the conditions for APD suppression identified by Li and co-workers^{13,14} are likely to result in significant Ge outdiffusion, and further work is required to identify MOCVD growth conditions which simultaneously produce APD suppression and chemically sharp interfaces. The best MOCVD material^{13,14} has been grown using initial arsine exposure. In contrast, it has been reported that when using gas-source MBE (cracked arsine and a Ga effusion furnace) a Ga prelayer is required to obtain good GaAs material on a thick Ge film grown on a Si substrate.^{29–31} Mizuguchi *et al.*²¹ reported that the use of off-orientated (100) Ge substrates is essential for the successful growth of single-domain GaAs epitaxial layers on Ge (100) by MOCVD. They found that the GaAs layers on 2° off (100) Ge substrates are of high quality by using x-ray rocking curves and 4.2 K photoluminescence measurement. Timo *et al.*¹⁵ used the Ge crystal 6° off (100) toward [110] for GaAs growth by low-pressure metal–organic vapor-phase epitaxy (LP-MOVPE) because vicinal substrates are, indeed, known to avoid APDs formation and to reduce threading dislocation generation.^{16,32} Most recently, Timo *et al.*³³ used Ge substrates whose orientation was (100) 9° off towards [111] for AlGaAs/GaAs/Ge solar cells by LP-MOVPE. Several groups have used (100) substrates misoriented towards [011] to grow GaAs, which is free of APDs.^{17,21} Lazzarini *et al.*¹⁹ used *n*-type Ge substrates, with a miscut angle ranging from 0° to 4° off (001) towards [111] for single-crystal GaAs epitaxial layers by the atmospheric MOVPE technique. They found that 3° misorientation of the substrate is effective in suppressing the formation of APDs, but only in optimized growth conditions. Few reports^{15,33,34} on Si-doped GaAs on Ge are available for indirect information on the interdiffusion phenomena by PL investigations. Therefore, the selection of off-oriented Ge substrates for the deposition of GaAs epitaxial layers by LP-MOVPE is still controversial. There is no unique rule for optimal offset in the orientation of Ge substrates which could be used to suppress the APDs during the MOVPE growth of GaAs. The aim of this work is the detailed study of the growth temperature, V/III ratio, and growth rate effects on the Si-doped GaAs on Ge by photoluminescence spectroscopy for photovoltaic application, and these results are compared with Si-doped GaAs on GaAs substrates. The study leads to establishment of optimum growth conditions, which reproducibly generate GaAs films on Ge that are assumed to

be APDs free and which limit outdiffused Ge concentration of the GaAs/Ge heterointerface. The electron concentration increases with increasing growth temperatures, AsH₃, and TMGa mole fractions on Ge substrates, where the electron concentration increases with increasing growth temperature and decreases with increasing AsH₃ and TMGa mole fractions on GaAs substrates. A vacancy control model was found to be consistent with our AsH₃ variation on Ge substrates and TMGa variation on GaAs substrates. Finally, secondary ion mass spectroscopy (SIMS) results indicated nearly no or minimum Ge outdiffusion into GaAs epitaxial layers.

II. EXPERIMENT

Si-doped *n*-type GaAs were grown in each run in a low-pressure horizontal metal–organic vapor-phase epitaxy reactor on both Sb-doped *n*⁺-Ge (100) 6° off orientation towards the [110] direction and Cr-doped semi-insulating GaAs (100) substrates with an offset by 2° towards the [110] direction. The source materials were trimethylgallium (TMGa), (100%) arsine (AsH₃), (104 ppm) silane (SiH₄) as an *n*-type dopant, and palladium purified H₂ as a carrier gas. During the growth, the pressure inside the reactor was kept at 100 Torr and the growth temperature was varied from 600°C to 675°C . The TMGa and AsH₃ flow rate was varied from 5 to 15 SCCM and 30 to 100 SCCM, respectively. The total flow rate was about 2 SLPM. Prior to growth, the Ge substrates were degreased with organic solvents, then etched in 1HF:1H₂O₂:30H₂O for 15 s according to the specification given by the Ge substrate supplier, Laser Diode Inc.

PL measurements were carried out using a MIDAC Fourier transform PL (FTPL) system at a temperature of 4.2 K and 100 mW laser power. An argon ion laser operating at a wavelength of 5145 \AA was used as a source of excitation. The exposed area was about 3 mm^2 . A PL signal was detected by a LN₂-cooled Ge photodetector whose operating range is about 0.75–1.9 eV, while resolution was kept at about 0.5 meV. The doping concentrations were determined by using a Bio-Rad electrochemical capacitance voltage (ECV) polaron profiler. The interdiffusion near the heterointerface was investigated by secondary ion mass spectroscopy. A Cs⁺ ion was used as a primary ion with an acceleration energy of 10 keV.

III. RESULTS AND DISCUSSION

A. Effect of growth temperature on photoluminescence

Figure 1 shows the 4.2 K PL spectra obtained from the Si-doped GaAs epilayers on Ge substrates grown at different growth temperatures. The curves were intentionally offset along the y axis with respect to each other for better clarity. The same procedure was used for all other PL spectra in this paper. When the electron concentration is relatively low, the spectrum becomes symmetric, while higher electron concentrations lead to asymmetric spectra. The Si doping broadens the excitonic emission until it becomes a wide band-to-band (B–B) luminescence. The peak at 1.49 eV has been attributed to band-to-acceptor (B–A) transitions involving re-

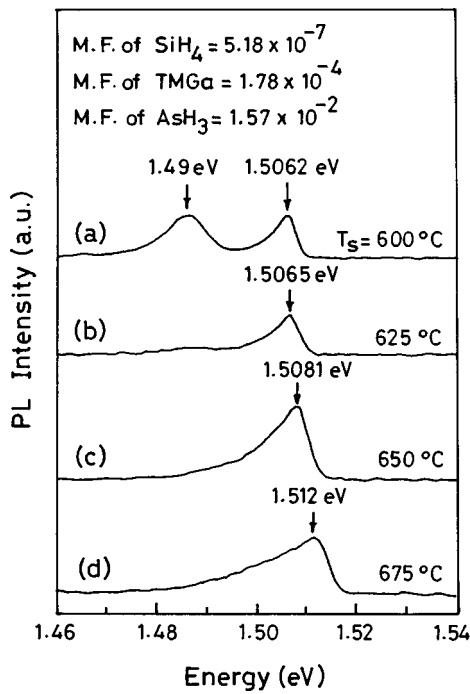


FIG. 1. Photoluminescence spectra of Si-doped GaAs epilayers grown under various growth temperatures on Ge substrates. The corresponding electron concentrations are: (a) $8 \times 10^{16} \text{ cm}^{-3}$, (b) $1.7 \times 10^{17} \text{ cm}^{-3}$, (c) $2.3 \times 10^{17} \text{ cm}^{-3}$, and (d) $5.7 \times 10^{17} \text{ cm}^{-3}$.

sidual carbon (C) impurities present in MOVPE GaAs.³⁵ The energy separation between the B–A peak and the B–B peak (band gap of GaAs at 4.2 K is 1.5194 eV) is consistent with typical acceptor ionization energies such as that of C ($E_a \sim 26.4 \text{ meV}$),³⁶ which is a *p*-type dopant in MOVPE. These B–A transitions are observed at growth temperatures $\leq 600^\circ \text{C}$ and decreases with increasing growth temperatures. From Fig. 1, it is seen that beyond the growth temperature, 625°C in our case, only one broad emission band is found, and the peak maximum of the dominant emission E_{max} is shifted monotonically towards higher energy with increasing free-carrier concentration. According to Burstein and Moss,³⁷ this shift results from the filling of the conduction band. The Burstein–Moss shift is more pronounced in *n*-type GaAs than *p*-type material because of the lower density of states at the bottom of the conduction band. The spectral shape of the main emission peak becomes strongly asymmetric having a steep slope on the high-energy side and a smooth slope on the low-energy side of the spectra. The asymmetry in the spectra of Fig. 1 at growth temperature $> 600^\circ \text{C}$ strongly indicates that indirect (without *k* selection) B–B or B–A transitions dominate the emission across the gap. The full width at half maximum (FWHM) of the B–B peak at 4.2 K of PL spectra increases with increasing growth temperatures. The electron concentration increases with increasing growth temperature on GaAs substrates, as can be seen from the Fig. 2. But the relative increase in PL peak energy is higher on GaAs substrates than on Ge substrates. The increase in PL peak shift towards higher energy corresponds to the increase in electron concentrations. The electron concentrations measured by an electrochemical capacitance voltage (ECV) profiler are mentioned in both the

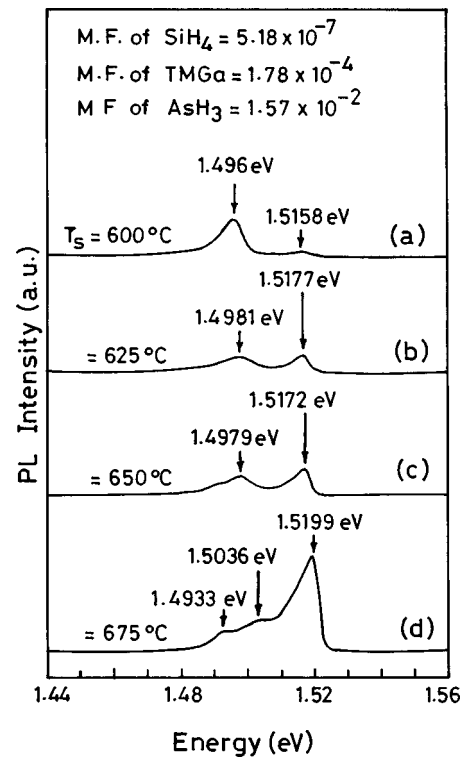


FIG. 2. Photoluminescence spectra of Si-doped GaAs epilayers grown under various growth temperatures on GaAs substrates. The corresponding electron concentrations are: (a) $1.3 \times 10^{17} \text{ cm}^{-3}$, (b) $2.45 \times 10^{17} \text{ cm}^{-3}$, (c) $3.64 \times 10^{17} \text{ cm}^{-3}$, and (d) $6.65 \times 10^{17} \text{ cm}^{-3}$.

figures for a better understanding of the growth process of Ge substrates. These features can be explained by assuming that the Burstein–Moss phenomenon is effective in the present layers and that the Si-doping efficiency in GaAs on GaAs substrates is higher than Si doping in GaAs on Ge substrates. A different level of Si incorporation in the GaAs on GaAs than Ge can be ruled out since the samples were grown at the same SiH_4 partial pressure. The role of Ge diffusion from the substrate into the epilayer is also ruled out because the Ge diffusion into the epilayer should increase the electron concentration. Masselink *et al.*²⁷ reported the first successful growth of GaAs and AlGaAs/GaAs superlattices on (100) Ge substrates. They performed photoluminescence measurements at 2 K on the AlGaAs/GaAs superlattices and on the GaAs bulk layers grown on (100) Ge. In all cases, the luminescence intensity was comparable to that of similar structures grown on GaAs, this suggests that there were few (if any) additional nonradiative centers or deep traps in the case of bulk GaAs grown on (100) Ge, the dominant photoluminescence feature is a single peak whose maximum lies between 1.477 and 1.473 eV depending on the excitation intensity. This luminescence is due to the $e\text{-Ge}_{\text{As}}^0$ and $\text{Ge}_{\text{Ga}}^0\text{-Ge}_{\text{As}}^0$ (free-electron-to-acceptor and donor-to-acceptor) transitions involving Ge from the substrate, and has a phonon replica at 1.437 eV. This would indicate a Ge binding energy in GaAs of 43 meV. They also observed the luminescence from the recombination of bound excitons at 1.511 eV. Mizuguchi *et al.*²¹ studied GaAs layers on (100) 2° off towards the [011] direction Ge and Si substrates by 4 K PL measurements. This PL has three bands, which are at 1.512

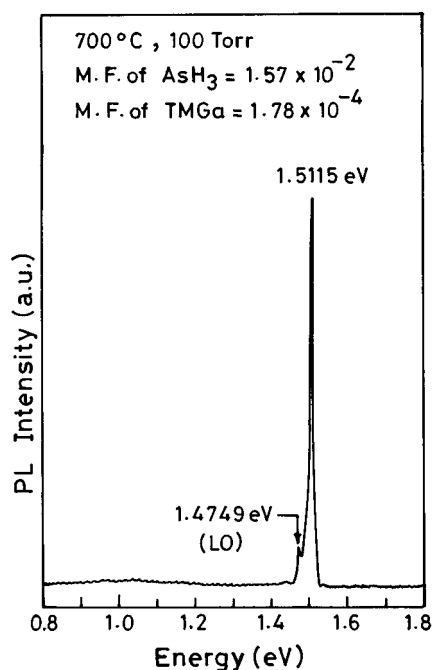


FIG. 3. Photoluminescence of undoped GaAs on Ge substrates.

eV corresponding to the acceptor-bound exciton, at 1.492 eV corresponding to the carbon acceptor band, and at 1.456 eV corresponding to the phonon replicate of the carbon acceptor band. The FWHM for the luminescence from excitons of the GaAs layer on 2° off (100) Ge is 7 meV, sharper than that of the GaAs layer on exactly (100) Ge, namely, 8.5 meV. Therefore, it is confirmed that the GaAs layer on 2° off (100) Ge is of higher quality than that on the exactly (100) Ge substrate.

Before the intentional Si-doped GaAs on Ge growth, undoped GaAs on Ge ($\sim 2 \mu\text{m}$) were grown in order to check the Ge outdiffusion into the film. Figure 3 shows the PL spectrum of one of the GaAs layer on 6° off (100) toward the [110] Ge substrate. This PL has only one peak at 1.5115 eV corresponding to the acceptor-bound exciton which has a FWHM of 10.3 meV and at 1.4749 eV corresponding to the phonon replicate of the acceptor bound exciton band. This PL spectrum suggests that there is no Ge outdiffusion from the substrate, which is observed by Fischer *et al.*⁹ in the MBE growth process. Timo *et al.*,¹⁵ however, observed a massive diffusion of Ge into the epilayer by PL measurement in the low growth rate ($2 \mu\text{m/h}$) of the MOCVD process. The possible explanation for the increase in electron concentration in GaAs grown on GaAs substrates rather than Ge substrates in our case is the catalyzed pyrolysis of SiH_4 by the presence of a GaAs surface, while the polar and nonpolar nature of the substrates may cause the influence of silicon incorporation. The difference in electron concentration both on Ge and GaAs substrates could be the traps in the GaAs epilayer due to the defects originating from the heteroepitaxy. GaAs can be grown epitaxially on Ge in two equivalent orientations corresponding to an exchange of Ga and As sublattices.³⁸ Domains of differing orientation are separated by an antiphase boundary (APB). Since GaAs is a polar material, the APBs have a net charge and are expected to act as

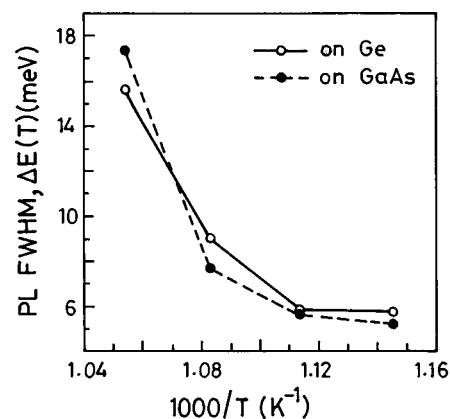


FIG. 4. FWHM of 4.2 K PL vs growth temperatures.

scattering centers.^{38,39} Antiphase boundaries in GaAs contain Ga–Ga and As–As bonds. Such bonds represent electrically charged defects, which may trap electrons.³⁸ This explanation becomes less likely at higher electron concentrations due to the required very high trap concentrations. Sieg *et al.*²⁰ observed identical Si-doping efficiencies on both GaAs and Ge substrates at least at low doping levels ($2.5 \times 10^{15} \text{ cm}^{-3}$) grown by the solid-source MBE technique. In addition, they also suggested that for MBE films, Ge outdiffusion into GaAs is an unlikely cause of the reduced apparent Si-doping efficiency, since Ge usually produces *n*-type doping in GaAs.

The full width at half maximum, $\Delta E(T)$ of the B–B peak at 4.2 K of the PL spectra increases with increasing electron concentrations in both cases (Fig. 4). But the relative increase in FWHM is more in the case of the Ge substrates than the GaAs substrates. This increase in FWHM in Ge substrates should imply an increase in electron concentration. Less electron concentration was found on the Ge substrates than the GaAs substrates. The FWHM relation with the electron concentration is an essential tool for the determination of electron concentration in Si-doped GaAs on both Ge and GaAs substrates.

B. Effect of AsH_3 variation on photoluminescence

To observe the effect of the V/III ratio on the optical properties of Si-doped GaAs on Ge, PL measurements were carried out at 4.2 K specifically on those samples grown at different AsH_3 flow rates. Figure 5 shows the PL spectra of Si-doped GaAs for fixed TMGa and SiH_4 mole fractions. The three curves represent three different AsH_3 flow rates. It is seen from Fig. 5 that the PL main peak energy shifted to higher photon energies with increasing AsH_3 mole fractions. In general, the formation of a GaAs epitaxial layer may be expressed as



and can be considered as a general equation during the growth of undoped GaAs. This ignores the possible presence of vacancies created during the growth. In addition, it is worth mentioning that the formation of GaAs is a very complex process and involves up to 17 gas-phase reactions.⁴⁰

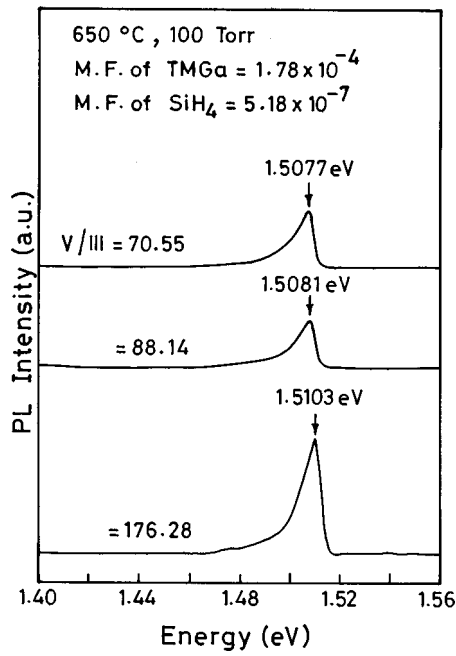
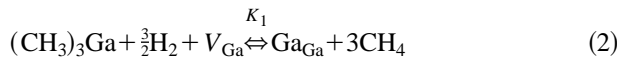


FIG. 5. 4.2 K PL spectra of Si-doped GaAs epilayers as a function of AsH_3 flow rate on Ge substrates.

The vacancies consideration in the lead reaction becomes significant during the process of doping incorporation, whether Zn for p type or Si for n -type doping. A vacancy-controlled model⁴¹⁻⁴³ may be considered to explain such behavior. In the TMGa- AsH_3 system, the leading reaction to the formation of GaAs can be expressed as



where K_1 and K_2 are the equilibrium constants of the above reactions, then

$$\frac{[V_{\text{Ga}}]}{[V_{\text{As}}]} \equiv \frac{K_2}{K_1} \frac{P_{\text{CH}_4}^3}{P_{\text{TMGa}}} \frac{P_{\text{AsH}_3}}{P_{\text{H}_2}^3}. \quad (4)$$

Since Si as a donor is on the Ga sublattice, under equilibrium its incorporation should be proportional to the concentration of Ga vacancies, V_{Ga} .⁴⁴ The doping reaction is



From Eqs. (4) and (5) one can write,

$$\frac{[\text{Si}_{\text{Ga}}]}{[V_{\text{As}}]} \equiv \frac{K_2 K_3}{K_1} \frac{P_{\text{SiH}_4}}{P_{\text{TMGa}}} \frac{P_{\text{AsH}_3}}{P_{\text{H}_2}^3} P_{\text{CH}_4}^3. \quad (6)$$

An increase in P_{AsH_3} will increase in gallium vacancy concentration, hence, the incorporation of Si on Ga sites is increased. The electron concentration is, thus, increased when the AsH_3 mole fraction is increased, and hence, the PL main peak is shifted towards the higher energy with increasing AsH_3 mole fraction. According to Li and co-workers,^{13,14} the conditions for the suppression of APDs are either the increase in a higher V/III ratio or a lower growth rate (i.e.,

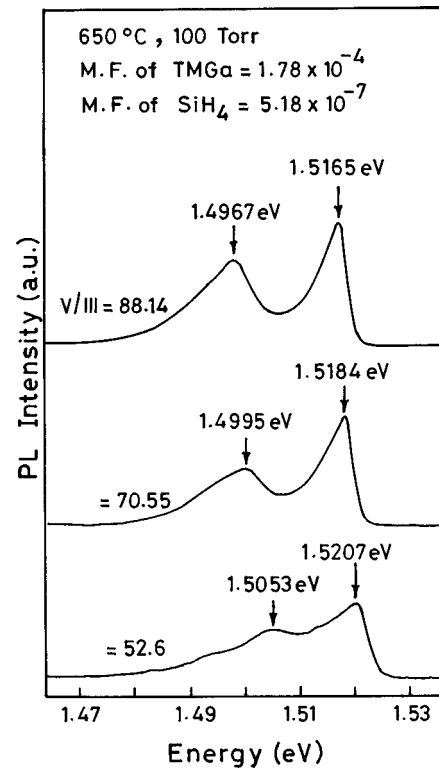


FIG. 6. 4.2 K PL spectra of Si-doped GaAs epilayers as a function of AsH_3 flow rate on GaAs substrates.

lower Ga flow). Since Ge diffuses into GaAs via Ga vacancies¹⁵ and the Ga vacancy population will increase with increasing V/III ratio and with decreasing growth rate, the Ge outdiffusion would be significant. This will be discussed in the TMGa variation case. There is some evidence in the literature that cracked AsH_3 can roughen the Ge surface, and a roughened surface leads to APDs and perhaps high dislocation densities, which in turn may produce high trap densities and less electron concentration.⁴⁵ However, we also studied the optical properties of low-doped layers grown with an increasing AsH_3 mole fraction to check if there is an amphoteric effect of Si on GaAs substrates. Figure 6 shows the PL spectra of Si-doped GaAs for fixed TMGa, SiH_4 mole fractions. It is seen from Fig. 6 that the PL main peak energy shifted to lower photon energies since the electron concentration decreases with increasing AsH_3 mole fractions. The electron concentration decreases with the increasing V/III ratio for a given TMGa mole fraction and growth temperature of Si-doped GaAs, which is the same as described by Bass.⁴⁴ According to the above model, as the AsH_3 concentration is increased, the V_{Ga} concentration increases, and therefore, the Si donor level should also increase. Conversely, as the AsH_3 concentration decreases, the As vacancies should increase and the Si as an acceptor should increase. The fact that the reverse behavior takes place suggests that the incorporation of Si is not controlled by the bulk thermodynamic properties of the lattice but by the surface kinetics process; the As appears to block the Si from the growing surface.⁴⁴ But, we found that for a fixed concentration of the SiH_4 mole fraction the electron concentration decreases with increasing AsH_3 concentration. At a V/III ratio of 52.6, the growth-induced

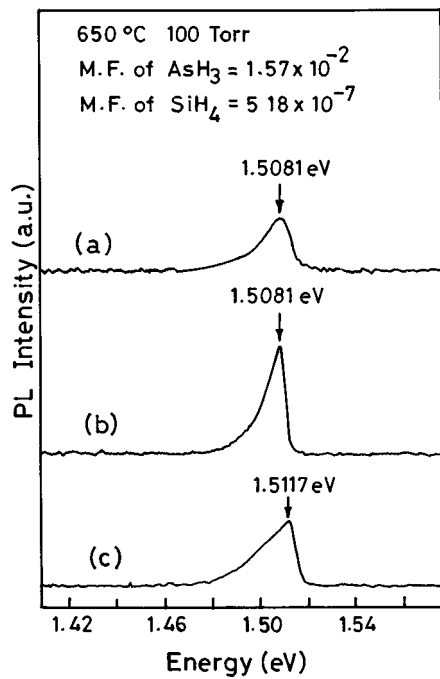


FIG. 7. 4.2 K PL spectra of Si-doped GaAs epilayers as a function of TMGa flow rate on Ge substrates. The TMGa mole fractions are: (a) 8.88×10^{-5} , (b) 1.78×10^{-4} , and (c) 2.68×10^{-4} .

point defects at 1.5053 eV called the Künzel–Ploog defect exciton was observed similar to that observed in MBE grown GaAs as discussed by Künzel and Ploog.⁴⁶ Even at this V/III ratio, the conduction-band-to-acceptor (C–A) or donor-to-acceptor (D–A) transition is not observed whereas it is frequently found at MOVPE grown GaAs. From these observations and from Hall mobility data, the lightly doped layers were not caused by the amphoteric nature of Si. On the other hand, the peaks at 1.4967 eV and 1.4995 can influence the electrical properties of lightly doped layers. These peaks may be attributed to Zn and C (2S), respectively. The peak is asymmetric at a lower AsH₃ mole fraction and becomes symmetric at a higher AsH₃ mole fraction.

C. Effect of TMGa variation on photoluminescence

To observe the effect of the TMGa mole fraction on the optical properties of Si-doped GaAs, PL measurements were carried out at 4.2 K specifically on those samples grown at different TMGa flow rates. Figure 7 shows the PL spectra of Si-doped GaAs for fixed AsH₃ and SiH₄ mole fractions. The three curves represent three different TMGa flow rates. It is seen from Fig. 7 that the PL main peak energy shifted to higher photon energies with increasing TMGa mole fractions. However, a different observation was found in Si-doped GaAs on Cr-doped semi-insulating GaAs (100) substrates. In this case, the PL main peak energy shifted to higher photon energy with decreasing TMGa flow rates (Fig. 8), since the electron concentration decreases with increasing TMGa mole fractions. From Eq. (5) we found that the decrease in P_{TMGa} will increase in Ga-vacancy concentration. Since Si incorporates in the Ga site and gives an *n* type, the electron concentration increases with decreasing TMGa flow

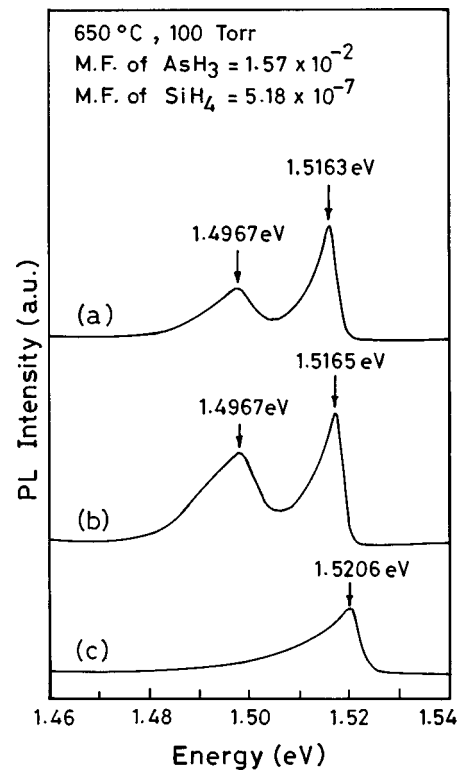


FIG. 8. 4.2 K PL spectra of Si-doped GaAs epilayers as a function of TMGa flow rate on GaAs substrates. The TMGa mole fractions are: (a) 2.68×10^{-4} , (b) 1.78×10^{-4} , and (c) 8.88×10^{-5} .

rates, and hence, the PL peak energy shifted to higher photon energy. A possible explanation in the former case may be the increase in Ga interdiffusion in Ge with increasing TMGa, i.e., increasing growth rate, and creates more Ga vacancies in the epitaxial film, and hence, Si incorporation increases. In order to check the interdiffusion of Ga into Ge and as well as the Ge outdiffusion into GaAs films the secondary ion mass spectroscopy technique was used. It is a powerful technique for quantitative measurements of dopant and impurity levels in semiconductors.⁴⁷ The concentration of a particular element can be profiled through a layer using the dynamic SIMS technique. In this method, the mass spectral peak intensity corresponding to a particular ion is monitored as function of time using a high sputtering rate. Figure 9 shows depth profiles ($\approx 15 \text{ \AA/s}$) of Ga, As, Ge, C, Si, and O atoms in the Si-doped GaAs on Ge, measured by SIMS for a TMGa mole fraction of 1.78×10^{-4} . All atoms were hardly interdiffused at the heterointerface of the GaAs–Ge (100) substrate. The abrupt heterointerface in this film indicates almost no outdiffusion of Ge into the GaAs epilayer. Since there is no outdiffusion of Ge into the GaAs epitaxial layer, the increase in electron concentration with increasing AsH₃ partial pressure could be explained by the vacancy-controlled model. An increase in carrier concentration was also observed with the increasing TMGa mole fraction, which is in contradiction to that behavior observed in the case of the GaAs substrates. More systematic data are felt to be necessary to explain such behavior, which is in progress.

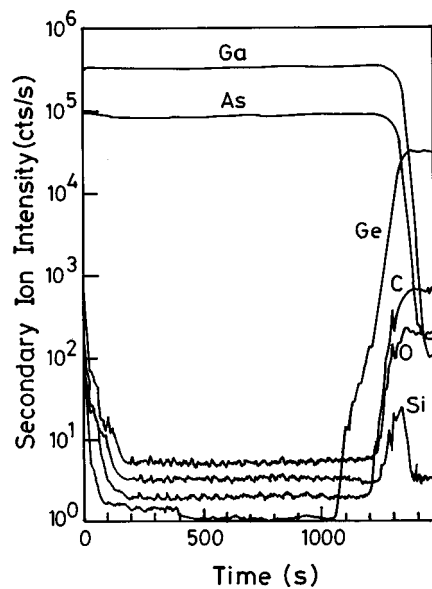


FIG. 9. SIMS depth profiles of compositional atoms around the heterointerface between the Si-doped GaAs epilayer and the Ge (100) substrate (sputtering rate $\approx 15 \text{ \AA}^2/\text{s}$).

IV. CONCLUSIONS

Si-doped GaAs epitaxial layers grown by low-pressure metal-organic vapor-phase epitaxy on Ge have been investigated by photoluminescence spectroscopy as a function of growth temperature, AsH_3 , and TMGa mole fraction. The B-B peak shifts to higher energy with increasing growth temperature, i.e., increasing electron concentrations due to a Burstein-Moss shift. Band-acceptor transitions involving residual C acceptors are the dominant recombination processes at growth temperatures below $600 \text{ }^\circ\text{C}$. Above $600 \text{ }^\circ\text{C}$, however, the dominating contribution to the spontaneous recombination process in *n*-type GaAs arises from (indirect) transitions between free electrons in the conduction band and localized acceptorlike centers in the deeper tail states above the valence-band edge. The B-B peak also shifts to high energy as the AsH_3 and TMGa mole fractions increase on Ge substrates and shift to lower energy when grown on GaAs substrates. This may be due to the enhanced pyrolysis of SiH_4 on the GaAs surface or due to antiphase domains or high dislocation densities from the heteroepitaxy. A comparative study of Si doping in GaAs on both Ge and GaAs substrate surfaces by low-temperature photoluminescence spectroscopy has been investigated. The peak shift towards the higher-energy side with increasing AsH_3 variation has been explained by the vacancy-controlled model. Almost no outdiffusion of Ge takes place during MOVPE growth of GaAs on Ge substrates.

ACKNOWLEDGMENTS

The authors wish to thank Dr. K. S. R. K. Rao for PL measurements and R. Ashwatraman, IGCAR, Kalpakkam for SIMS analysis.

¹R. A. Metzger, *Compound Semicond.* **2**, 25 (1996).

²M. Kato, K. Mitsui, K. Mizuguchi, N. Hayafuji, S. Ochi, Y. Yukimoto, T.

- Murotani, and K. Fujikawa, Proceedings of the 18th IEEE Photovolt. Spec. Conference, Las Vegas (1985), p. 14.
- ³C. Flores, D. Passoni, and G. Timò, Proceedings of the European Space Power Conference, Spain ESA SP-294 (1989), p. 507.
- ⁴C. Flores, B. Bollani, R. Campesato, F. Paletta, D. Passoni, G. Timò, and A. Tosoni, *Sol. Energy Mater.* **23**, 356 (1991).
- ⁵K. I. Chang, Y. C. M. Yeh, P. A. Iles, J. M. Tracy, and R. K. Morris, Proceedings of the 19th IEEE Photovoltaic Spec. Conference (1987), p. 273.
- ⁶P. A. Iles, Y. C. M. Yeh, F. H. Ho, C. L. Chu, and C. Cheng, *IEEE Electron Device Lett.* **EDL-11**, 140 (1990).
- ⁷N. Chand, J. Klem, and H. Morkoç, *Appl. Phys. Lett.* **48**, 484 (1986).
- ⁸S. C. Martin, L. M. Hitt, and J. J. Rosenberg, *IEEE Electron Device Lett.* **EDL-10**, 325 (1989).
- ⁹R. Fischer, W. T. Masselink, J. Klem, T. Henderson, T. C. McGlenn, M. V. Klein, H. Morkoç, J. H. Mazur, and J. Washburn, *J. Appl. Phys.* **58**, 374 (1985).
- ¹⁰A. G. Milnes and D. L. Feucht, in *Heterojunctions and Metal-Semiconductor Junctions* (Academic, New York, 1972), p. 58.
- ¹¹C. Flores, B. Bollani, R. Campesato, D. Passoni, and G. L. Timò, *Microelectron. Eng.* **18**, 175 (1992).
- ¹²S. J. Wojtczuk, S. P. Tobin, C. J. Keavney, C. Bajgar, M. M. Sanfacon, L. M. Geoffroy, T. M. Dixon, S. M. Vernon, J. D. Scofield, and D. S. Ruby, *IEEE Trans. Electron Devices* **ED-37**, 455 (1990).
- ¹³Y. Li, L. Lazzarini, L. J. Giling, and G. Salviati, *J. Appl. Phys.* **76**, 5748 (1994).
- ¹⁴Y. Li, G. Salviati, M. M. G. Bongers, L. Lazzarini, L. Nasi, and L. J. Giling, *J. Cryst. Growth* **163**, 195 (1996).
- ¹⁵G. Timò, C. Flores, B. Bollani, D. Passoni, C. Bocchi, P. Franzosi, L. Lazzarini, and G. Salviati, *J. Cryst. Growth* **125**, 440 (1992).
- ¹⁶S. Strite, D. Biswas, N. S. Kumar, M. Fradkin, and H. Morkoç, *Appl. Phys. Lett.* **56**, 244 (1990).
- ¹⁷P. R. Pukite and P. I. Cohen, *J. Cryst. Growth* **81**, 214 (1987).
- ¹⁸K. Morizane, *J. Cryst. Growth* **38**, 249 (1977).
- ¹⁹L. Lazzarini, Y. Li, P. Franzosi, L. J. Giling, L. Nasi, F. Longo, M. Urchulutegui, and G. Salviati, *Mater. Sci. Eng. B* **28**, 502 (1992).
- ²⁰R. M. Sieg, S. A. Ringel, S. M. Ting, and E. A. Fitzgerald, *J. Electron. Mater.* (submitted).
- ²¹K. Mizuguchi, N. Hayafuji, S. Ochi, T. Murotani, and K. Fujikawa, *J. Cryst. Growth* **77**, 509 (1986).
- ²²T. Kawai, H. Yonezu, H. Yoshida, and K. Pak, *Appl. Phys. Lett.* **61**, 1216 (1992).
- ²³T. Kawai, H. Yonezu, Y. Yamauchi, M. Lopez, and K. Pak, *J. Cryst. Growth* **127**, 107 (1993).
- ²⁴N. Chand, J. Klem, T. Henderson, and H. Morkoç, *J. Appl. Phys.* **59**, 3601 (1986).
- ²⁵R. L. Anderson, *Solid-State Electron.* **5**, 341 (1962).
- ²⁶D. L. Miller and J. S. Harris, Jr., *Appl. Phys. Lett.* **37**, 1104 (1980).
- ²⁷W. T. Masselink, R. Fischer, J. Klem, T. Henderson, P. Pearah, and H. Morkoç, *Appl. Phys. Lett.* **45**, 457 (1984).
- ²⁸P. M. Petroff, A. C. Gossard, A. Savage, and W. Wiegmann, *J. Cryst. Growth* **46**, 172 (1979).
- ²⁹J. M. Kuo, E. A. Fitzgerald, Y. H. Xie, and P. J. Silverman, *J. Vac. Sci. Technol. B* **11**, 857 (1993).
- ³⁰E. A. Fitzgerald, J. M. Kuo, Y. H. Xie, and P. J. Silverman, *Appl. Phys. Lett.* **64**, 733 (1992).
- ³¹Q. Xu, J. W. P. Hsu, E. A. Fitzgerald, J. M. Kuo, Y. H. Xie, and P. J. Silverman, *J. Electron. Mater.* **25**, 1009 (1996).
- ³²R. Fischer, H. Morkoç, D. A. Neuman, H. Zabel, C. Choi, N. Otsuka, M. Longebone, and L. P. Erickson, *J. Appl. Phys.* **60**, 1640 (1986).
- ³³G. Timò, L. Solevi, and T. H. Njung, *Mater. Sci. Eng. B* **28**, 474 (1994).
- ³⁴G. L. Timò and C. Flores, Proceedings of the 1st IEEE World Conference on Photovoltaic Energy Conversion, Hawaii (1994), p. 2200.
- ³⁵V. Swaminathan, D. L. Van Haren, J. L. Zilko, P. Y. Lu, and N. E. Schumaker, *J. Appl. Phys.* **57**, 5349 (1985).
- ³⁶D. J. Ashen, P. J. Dean, D. T. J. Hurle, J. B. Mullin, and A. M. White, *J. Phys. Chem. Solids* **36**, 1041 (1975).
- ³⁷E. Burstein, *Phys. Rev.* **93**, 632 (1954); T. S. Moss, *Proc. Phys. Soc. London, Sect. B* **67**, 775 (1954).
- ³⁸H. Kroemer, *J. Cryst. Growth* **81**, 193 (1987).
- ³⁹P. M. Petroff, *J. Vac. Sci. Technol. B* **4**, 874 (1986).
- ⁴⁰T. J. Mountziaris and K. F. Jensen, *J. Electrochem. Soc.* **138**, 2426 (1991).
- ⁴¹Y. K. Su, C. Y. Chang, T. S. Wu, Y. C. Chou, and C. Y. Nee, *J. Cryst. Growth* **67**, 472 (1984).

⁴²C. Y. Chang, L. P. Chen, and C. H. Wu, *J. Appl. Phys.* **61**, 1860 (1987).

⁴³N. Putz, H. Heinecke, M. Heyen, and P. Balk, *J. Cryst. Growth* **74**, 292 (1986).

⁴⁴S. J. Bass, *J. Cryst. Growth* **47**, 613 (1979).

⁴⁵N. Chand, F. Ren, A. T. Macrander, J. P. van der Ziel, A. M. Sergent, R.

Hull, S. N. G. Chu, Y. K. Chen, and D. V. Lang, *J. Appl. Phys.* **67**, 2343 (1990).

⁴⁶H. Künzel and K. Ploog, *Appl. Phys. Lett.* **37**, 416 (1980).

⁴⁷C. R. Brundle, C. A. Evans, and S. Wilson, *Encyclopedia of Materials Characterization* (Butterworth-Heinemann, CT, 1992).